

Seismic Oceanography

A New Tool to Characterize Physical Oceanographic Structures and Processes

Grant George Buffett

ADVERTIMENT. La consulta d'aquesta tesi queda condicionada a l'acceptació de les següents condicions d'ús: La difusió d'aquesta tesi per mitjà del servei TDX (www.tesisenxarxa.net) ha estat autoritzada pels titulars dels drets de propietat intel·lectual únicament per a usos privats emmarcats en activitats d'investigació i docència. No s'autoritza la seva reproducció amb finalitats de lucre ni la seva difusió i posada a disposició des d'un lloc aliè al servei TDX. No s'autoritza la presentació del seu contingut en una finestra o marc aliè a TDX (framing). Aquesta reserva de drets afecta tant al resum de presentació de la tesi com als seus continguts. En la utilització o cita de parts de la tesi és obligat indicar el nom de la persona autora.

ADVERTENCIA. La consulta de esta tesis queda condicionada a la aceptación de las siguientes condiciones de uso: La difusión de esta tesis por medio del servicio TDR (www.tesisenred.net) ha sido autorizada por los titulares de los derechos de propiedad intelectual únicamente para usos privados enmarcados en actividades de investigación y docencia. No se autoriza su reproducción con finalidades de lucro ni su difusión y puesta a disposición desde un sitio ajeno al servicio TDR. No se autoriza la presentación de su contenido en una ventana o marco ajeno a TDR (framing). Esta reserva de derechos afecta tanto al resumen de presentación de la tesis como a sus contenidos. En la utilización o cita de partes de la tesis es obligado indicar el nombre de la persona autora.

WARNING. On having consulted this thesis you're accepting the following use conditions: Spreading this thesis by the TDX (www.tesisenxarxa.net) service has been authorized by the titular of the intellectual property rights only for private uses placed in investigation and teaching activities. Reproduction with lucrative aims is not authorized neither its spreading and availability from a site foreign to the TDX service. Introducing its content in a window or frame foreign to the TDX service is not authorized (framing). This rights affect to the presentation summary of the thesis as well as to its contents. In the using or citation of parts of the thesis it's obliged to indicate the name of the author.

Estructura i Dinàmica de la Terra
Institut de Ciències de la Terra "Jaume Almera"
Consejo Superior de Investigaciones Científicas (CSIC)

Departament de Geodinàmica i Geofísica
Universitat de Barcelona

Seismic Oceanography

A New Tool to Characterize Physical Oceanographic Structures and Processes

Memòria presentada per Grant George Buffett per optar al Títol de Doctor en Geologia

Aquesta tesi ha estat realitzada dins el Programa de Doctorat Exploració, Anàlisi i modelització de conques i sistemes orogènics bienni 2006-2008, de la Universitat de Barcelona.

Director:

Prof. Dr. Ramón Carbonell i Bertrán

Tutor:

Dra. Pilar Queralt i Capdevila

Grant George Buffett

Barcelona, Novembre de 2010

PART II.

Seismic Oceanography Background

CHAPTER 5

Multi-channel Seismic Reflection Profiling

*Science is the outcome of being prepared to live without certainty and
therefore a mark of maturity. It embraces doubt and loose ends.*

– A.C. Grayling

5.1 – Introduction

Multi-channel seismic (MCS) reflection profiling using the Common Midpoint (CMP) method has been practiced and ameliorated for several decades. The main contributor to its development historically has been the hydrocarbon industry in the interest of locating potential petroleum plays. In short, the method is this: by using multiple sound sources and sensitive receivers placed in known positions, a map of the subsurface can be generated based on the different manner in which sound reflects from different boundaries depending on their locations and physical characteristics. Consequently, precise observation of the reflected waves (their arrival time, intensity (amplitude), frequency and phase) can provide information on the locations and physical properties of the reflecting interfaces.

The first seismic surveys consisted of no more than an explosive source and a listening device located at some distance (offset) along the Earth's surface. The explosive source was assumed to generate sound (seismic) waves in all directions. Given that the angle of reflection of a wave is equal to its angle of incidence assuming no change in sound speed, the depth to the reflecting interface was calculated. More simply, one might consider a source and a receiver at an offset of zero such that the wave's raypath would be vertical. In this case, the angle of incidence and reflection would both be 0° , such that the depth (z) to the interface would be

$$z = \frac{t}{2} c_{sound} \quad , \quad \text{eq. 5.1}$$

where t is the travel time of the wave. The assumption here is that the speed of sound (c_{sound}) is known and invariant. This approach is flawed for two reasons: 1) the speed of sound is not well known in the subsurface and, 2) it cannot be said to be strictly constant. Moreover, in practice, considering both the source and receiver at zero-offset, the energy generated at the source contains enough unwanted signal (i.e. noise) to make the calculation of the arrival time of the reflected wave untenable. For these and other reasons (to be discussed), other methodologies have been introduced to constrain variables, thereby increasing the accuracy of observation. Still, the most robust of the methods employed over time has been the CMP method (e.g. Sherriff, [1995]; Yilmaz, [2001]).

In practice, seismic reflection profiling proceeds in four stages: survey design, acquisition, analysis (data processing) and interpretation. The design stage involves choosing the site to perform the experiment and the acquisition parameters considered necessary for optimal imaging. Many factors have to be taken into account, from topographic or morphological conditions (on land surveys) to cultural and environmental conditions as well as permission to acquire data. For marine surveys, of which this thesis is concerned, the planning stage may involve potential conflicts over fishing or commercial rights in international or coastal waters. For seismic oceanography in particular, one must know what oceanic target is of interest and whether this target is viable given the acquisition equipment. A well planned survey can avoid problems at later stages. But a survey rarely, if ever, goes according to plan. There are usually unforeseen circumstances which require impromptu logistical or implementation changes. Digital processing and analysis of seismic data follows from a well designed and well implemented survey. Cooperation between field crews and processing scientists is of the utmost importance. Many times human or other errors that occur during acquisition can be accounted for if properly noted. Modern surveys are performed with solid state electronics and record any changes to the acquisition, making that information available to the data processor.

Data processing transforms interpretively useless data into an image of the subsurface. The interpretation of seismic data depends upon knowledge of all previous stages as well as having knowledgeable persons at hand whom descriptively understand the target (e.g. a geologist or oceanographer). An accurate, informative interpretation can only result from a well planned, well executed and correctly processed data set. The following three subsections discuss the acquisition, processing and interpretation of seismic reflection data. Focus will be on seismic reflection methods in reference to physical oceanography with the exception of some historical background of other surveys.

The goal of this chapter is not to author a complete treatise on seismic reflection methods. However, the following sections describe in detail the fundamentals of multi-channel (MCS) profiling against the framework of physical oceanographic structures and processes. That is, it will center on what we can expect to image using modern

technology in light of what has already been imaged by previous authors and, given what has been learned, what might be legitimate targets for future surveys.

5.2 – Governing equations of seismic wave propagation

Sound, fundamentally, is the mechanical vibration of a substance as a result of force. It is the oscillation of pressure in an elastic medium (this discourse will focus on body waves, or those internal to a medium). Considering a simple point force in a homogeneous, isotropic medium, the vibration diverges from the point source spherically. The vibration of a medium can be perpendicular, parallel or at some angle to the direction of wave propagation. Waves that oscillate parallel to the direction of propagation are called compressional waves (P-waves) and waves which oscillate perpendicular to the direction of propagation are termed shear waves (S-waves). To a large degree, the ocean acts as a perfect fluid. S-waves do not propagate in fluids because they require that the medium be able to sustain shear deformation with no change in volume [Kennett, 2001]. Thus, the text will thus exclusively refer to P-waves in the ocean.

The wave equation describes all wave propagation, from electromagnetic waves, to sound waves and those of fluid dynamics. Here, we describe acoustic waves, the simplest form of the wave equation being

$$\nabla^2 \varphi = \frac{1}{c^2} \frac{\partial^2 \varphi}{\partial t^2} \quad , \quad \text{eq. 5.2}$$

where φ is defined as

$$\varphi = A e^{i(\mathbf{k} \cdot \mathbf{x} - \omega t)} \quad , \quad \text{eq. 5.3}$$

and A is amplitude, \mathbf{k} is the wave vector, \mathbf{x} is the position vector and the combination $(\mathbf{k} \cdot \mathbf{x} - \omega t)$ represents the wave's phase. The symbol c is sound speed independent of position, and t is time [Chapman, 2004].

When a plane wave is incident on a boundary⁴, a portion of energy is transmitted and a portion reflected. Partitioning of wave energy at a boundary is described by Chapman [2004] by its slowness vector $\mathbf{p}=\mathbf{k}/\omega$, which leads to the reflection law

$$\theta_{inc} = \theta_{refl} \quad , \quad \text{eq. 5.4}$$

and Snell's law for the refracted, transmitted wave,

$$\frac{\sin \theta_{inc}}{c_1} = \frac{\sin \theta_{trans}}{c_2} \quad . \quad \text{eq. 5.5}$$

5.3 – Acquisition

Seismic reflection profiling has been successfully used for decades to image the subsurface of the earth. It is a well tested method first described by Reginald Fessenden and developed by the hydrocarbon industry to aid in the exploration of oil and gas [Finch, 1985]. Initial surveys in the first part of the 20th century involved one shot and one receiver on the surface with a known separation (offset). The time from the first shot to the first detection of upgoing energy in the receiver was used to calculate the depth to the reflecting interface. However, many assumptions were needed to make this calculation. The subsurface was considered to be homogeneous and isotropic and the reflecting interface, horizontal. Furthermore, the depth to the interface, relative to the source-to-receiver separation was assumed to be very large, thus approximating the source and receiver to be effectively co-located, thereby measuring a near zero-offset reflection. Although replete with assumptions, the method allowed the first proof-of-concept for seismic reflection.

Marine seismic reflection surveys are done by a large ship towing an impulsive source and a streamer (a cable filled with hydrophones) which record both signal and noise (Figure 5.1). The acoustic energy travels through the water column and the Earth's crust, while becoming attenuated and losing energy through spherical divergence. Acoustic impedance boundaries, defined by varying density and sound speed, determine

⁴ Boundaries for the propagation of sound are termed 'acoustic impedance boundaries' and for the purposes of this discourse in reference to seismic oceanography, represent isopycnals.

the transmission to reflection ratio. Transmitted energy is absorbed by the ocean and solid earth and is attenuated as it is converted to other forms of energy (e.g. kinetic energy, heat). Reflected energy, also being attenuated somewhat, is recorded by the towed streamer and stored for later processing.

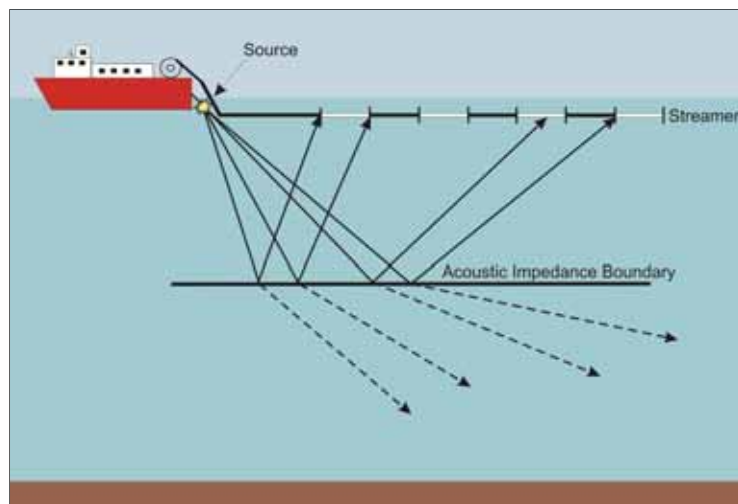


Figure 5.1 - Marine seismic acquisition in seismic oceanography showing reflected and transmitted waves.

It should be noted at this point that seismic reflection profiling over the ocean does not represent a true snapshot as it would for the solid Earth. This is because ocean dynamics are such that significant disruption can take place to the thermohaline finestructure that data recorded at the beginning of the seismic section and those recorded at the end can be separated in time by many hours or even days, depending on the length of the section to be acquired (Figure 5.2). Thus, caution should be practiced during interpretation of the data. Seismic oceanography 2D sections ('snapshots') are more properly defined as 2D+time quasi snapshots of a progressively changing ocean.

5.3.1 – Marine Seismic Sources and Receivers

In marine seismic surveys, dynamite has been long replaced by airguns as the source. Airguns release a known volume of compressed air into the water column. The advantage of airguns is that they are less invasive on marine ecosystems, less expensive and more predictable in terms of source pulse signature. Impulsive sources have a

distinct wavelet shape, which is characterized by the majority of the energy being front-loaded, that is, confined to the beginning of the wavelet, with a quickly decaying coda. This is referred to as minimum phase [Yilmaz, 1987]. This contrasts with some land surveys which use large vibrators (Vibroseis™) that generate a center-loaded wavelet shape (zero-phase) with the dominant energy contained in the center of the pulse.

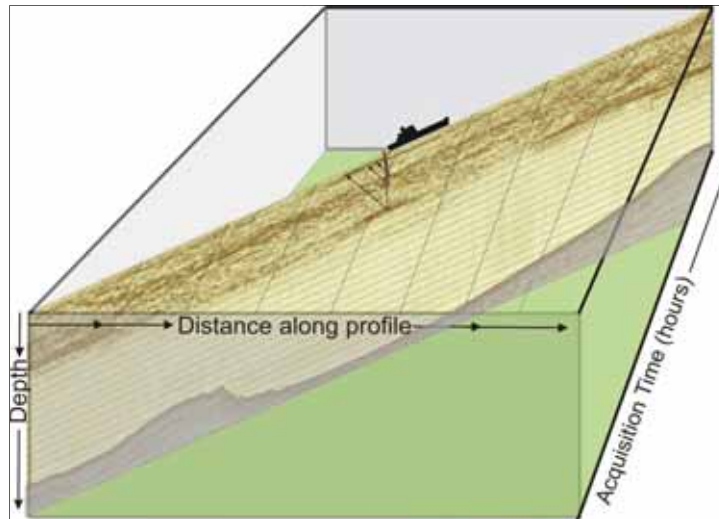


Figure – 5.2 - Diagram showing how a seismic oceanography section is skewed in time. This is an important point to remember during interpretation.

Source strength is directly related to the volume of compressed air in the chamber of an airgun, the physical shape of the gun, the air pressure and the hydrostatic pressure [Géli et al., 2009]. The chamber is filled with high air pressure and the compressed air is then released by an electrical signal, which operates a solenoid switch causing an imbalance in the pressures across a shuttle valve [Hobbs, 2007].

In seismic oceanography, given the weakness of reflectivity due to small acoustic impedance contrasts, a larger source may be preferable to obtain satisfactory signal-to-noise ratio. This is illustrated well in the imaging success of the IAM survey in seismic oceanography (e.g. Biescas et al. [2008]; Krahmman et al. [2008]; Buffett et al. [2009]; Ruddick et al. [2009]). However, larger sources are generally biased toward lower frequencies, thus reducing the resolving power of the signal. Smaller sources generate

higher frequencies, but are narrower bandwidth. Thus, a source balance needs to be found that is region and target independent, a task that may be difficult in practice.

One of the objectives of the GO project was to test different sources to determine which were most useful to seismic oceanography in terms of source strength, effective resolution and signal-to-noise ratio. Géli et al. [2009] reported that the small volume (117 cu-inch; ≈ 2 liters) mini-GI gun provided high resolution data but relatively low signal-to-noise ratio. Higher frequencies are more effectively attenuated by a given medium and thus do not achieve as much depth of penetration as lower frequency sources. Furthermore, while for MCS reflection studies of the solid Earth, there is little to no transition zone between acoustic impedance interfaces (since rocks are more abruptly juxtaposed against one another than thermohaline contrasts of water masses), in the ocean, there is heat and mass diffusion across interfaces which produces a more gradual change over a finite boundary width of tens of meters. As a result, the gradient of the water mass boundary makes the reflectivity frequency dependent [Hobbs et al., 2009].

During the GO project, in addition to independent low and high-frequency surveys, a multi-frequency source was used. This consisted of two separate airgun arrays with three airguns in each array. The result of this gun arrangement produced a source wavelet with a frequency response between 8 and 55 Hz for the low-frequency component and a 12-120 Hz range for the high-frequency array [Hobbs et al., 2009]. The result of this combination of sources was clear. The multi-frequency dataset showed that in comparison with single-source bandwidths (that only provide partial information on the structure in question), there is a wider range of spatial scales that can be imaged. Lower frequencies better image broader structures that are coherent over larger lateral distances, while higher frequencies delineate finer structures that may otherwise be missed, or misinterpreted [Hobbs et al., 2009] (Figure 5.3).

The first seismic receivers (geophones, or for marine surveys, hydrophones) were electromagnetic devices that operated by a magnet forced to oscillate vertically through a coil of wire by the reflected seismic wave, thus inducing a current which was then plotted as an analog time series. More recent receivers use piezoelectric materials to perform the same task. These receivers are distributed inside a rubber/plastic tube

(streamer), filled with a fluid (usually kerosene) to maintain neutral buoyancy. Streamers can vary in length between several hundred meters to over 10 km. Longer streamers allow more hydrophones (channels) to form a single shot record which permits longer offsets to be recorded, allowing better noise cancelation. In addition, each channel is composed of several hydrophones which sum together the received signal for the same purpose. Modern streamers are completely solid state with a foam filled interior for buoyancy. Attached to the streamer are 'birds', which are plastic winged devices that can be manually or automatically adjusted to position the streamer at the desired depth.

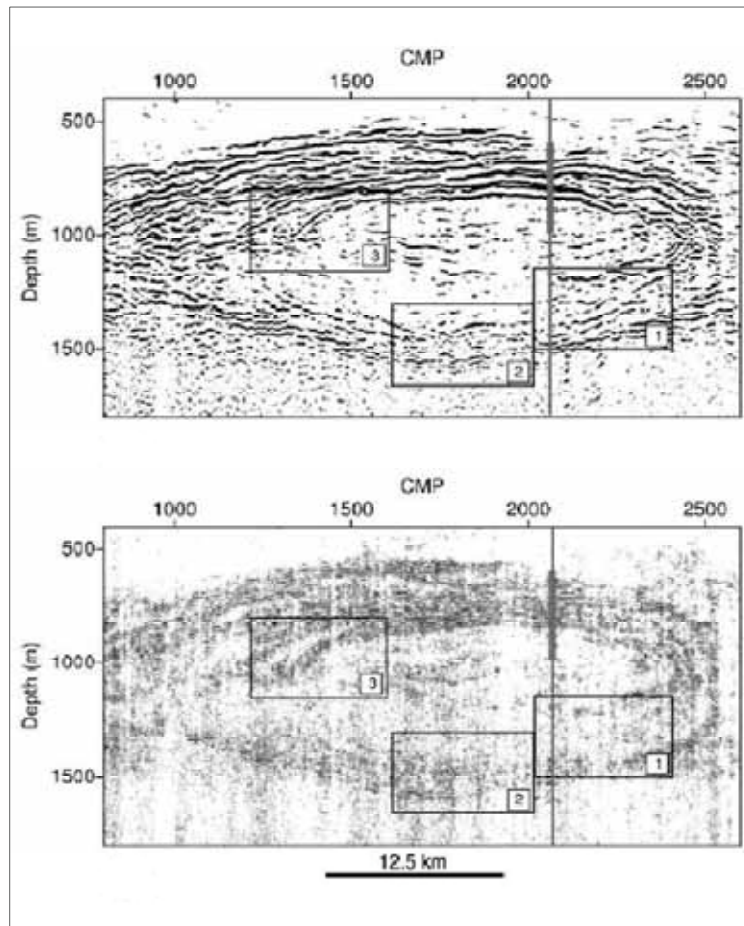


Figure 5.3 – Seismic images showing the effect of source bandwidth. Top image (10-40 Hz) shows broad structures across a range of depths, whereas the bottom image (40-120 Hz) reveals finer features, while not being as effective at greater depths. From Hobbs et al. [2009].

5.3.2 – The Common midpoint method

The common midpoint (CMP) method (Figure 5.4) of seismic acquisition design takes advantage of the redundancy of sources and receivers to produce a continuous image of the subsurface as well as to minimize noise. Instead of a single source and receiver, there is an array of sources and receivers at regular intervals with varying source-receiver offsets. The assumption is that time differences between individual traces within a CMP gather are not affected by structural differences [Cox, 1999]. This assumption is not strictly true in many cases, such as crooked-line surveys, and in marine surveys where the towed receiver streamer experiences 'feathering' due to near-surface currents. However, these effects are mostly accounted for with modern geometry deployments. In such cases 'binning' of midpoints is necessary to group common midpoints into user defined groups (or, bins). The objective of the CMP method is ultimately to approximate a zero-offset section (as if source and receiver were co-located), which is not possible in practice.

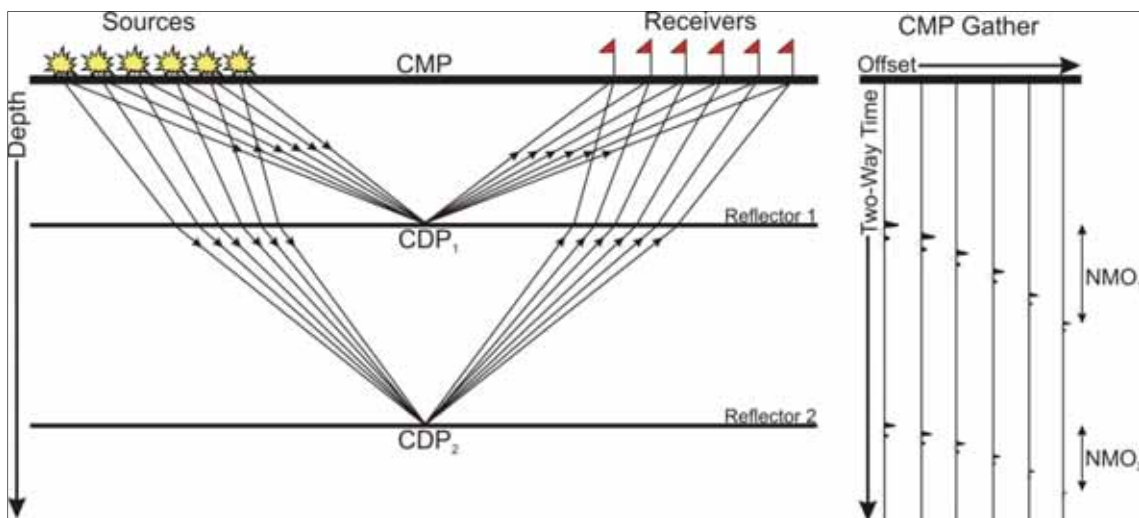


Figure 5.4 – The Common Midpoint Method (left) showing raypaths through different media, the Common Midpoint (CMP) between sources and receivers, Common Depth Point (CDP) of respective reflectors, and (right) CMP gather showing hyperbolic moveout of seismic traces with respect to offset and depth (travel time).

5.3.3 – *Specific challenges for seismic oceanography*

Some of the challenges for seismic oceanography acquisition are:

1) Ocean dynamics – As mentioned, a seismic oceanography acquisition snapshot is skewed by the nature of ocean dynamics. This poses a challenge for the interpreter. Given the velocity of ocean currents (on the order of tens to hundreds of centimeters per second) [Pedlosky, 1979], it is mistaken to expect a true snapshot of a large part of the ocean at any given time. The exception to this may be approached by observing spatially and temporally stable structures such as thermohaline staircases. These structures are observed in various regions of the oceans and have been imaged seismically (e.g. Fer et al. [2010]; Biescas et al. [2010]) and have been observed oceanographically to be 'quasi-permanent' in the deepest parts of the Tyrrhenian Sea (see Zodiatis and Gasparini [1996] and Figure 6.3).

2) Source bandwidth – As seen in Section 5.3.1, control over the source bandwidth is a determining factor to the proper imaging of thermohaline finestructure with suitable vertical and horizontal resolution. Seismic oceanography sources need to be properly customized to the region and target of interest. For example, for shallow targets, perhaps only a high-resolution source will suffice, while to image deeper structures, a combination might be employed. Moreover, the source impulse does not generate a simple bubble that expands and collapses neatly. The bubble's oscillation always adds noise to the source. This is compensated somewhat in Generator-Injector (GI) airguns, guns which are comprised of two separate air chambers. The Generator chamber produces the primary air bubble, whereas the Injector chamber is smaller and is used to attenuate the oscillation of the bubble after the primary collapse [Hobbs, 2007]. Proper estimation of the source signal is paramount to more complex seismic processing and modeling techniques [e.g. Papenberg et al., 2010].

5.4 – The seismic processor's toolbox

The goal of seismic data processing is to manipulate seismic data to yield an interpretable 2D slice or 3D volume of the subsurface. Accurate processing of seismic data requires certain tools, or operations. Some of these operations are necessary to data reduction and analysis, others are optional or may be data-dependent. The seismic processor benefits greatly from an in-depth understanding of the seismic data acquisition in order to choose wisely which tools to apply or which methods to test. The following is a description of some of the most important tools, with reference where necessary to their use in seismic oceanography.

5.4.1 – Digitization

Processing of seismic data starts with discrete sampling of the continuous analog signal into a digital waveform. This decomposition of the wavelet allows it to be represented as a decomposable time series such that the wavelet's characteristics (frequency, amplitude and phase) can be manipulated in precise ways. The more frequently the continuous signal is sampled, the more the resulting digital signal approaches the true analog signal. For the theoretical case of a zero sampling interval, the analog signal can be fully represented [Yilmaz, 1987]. Sampling of data at a smaller sampling rate than is useful to represent reality is unnecessary. Oversampling of data above a wisely chosen threshold, for example, may only introduce more noise and not benefit interpretation. In any case, oversampled data can simply be re-sampled at a lower rate later. However, one must particularly avoid undersampling the data, such as not to lose higher frequency field data above the Nyquist frequency, which is the maximum recoverable frequency bandwidth when digitizing data. When an analog signal is sampled into a discrete time series, the digital signal is reconstructed based on the number of samples. However, the reconstructed signal will inevitably lack the details from the analog signal, which are manifest in the higher frequency components [Yilmaz, 1987]. These higher frequency samples are not lost by digitization. They are folded-back or 'wrapped around' and appear as lower frequency components below the Nyquist frequency. The Nyquist frequency is expressed as

$$f_n = \frac{1}{2\Delta t} \quad , \quad \text{eq. 5.6}$$

where Δt is the sample rate. Therefore, if the analog signal is sampled at an interval of 2 ms, the maximum recoverable frequency is 250 Hz, whereas at 1 ms, frequencies up to 500 Hz can be recovered. The maximum temporal (vertical) resolution possible in the seismic data is a function of recoverable frequency and is generally agreed to be approximately one-quarter of the recoverable wavelength [Widess, 1973]. The coarser the sampling interval, the smoother is the digitized signal.

5.4.2 - The Fourier transform

The Fourier Transform is fundamental to seismic data analysis and applies to nearly all stages of processing. It converts a time series into its frequency domain representation and vice-versa [Sheriff, 1991]. Any given time series can be decomposed into its individual frequency components through the forward Fourier transform. Likewise, given the individual frequency components, a synthetic seismic trace can be constructed fully and completely through the inverse Fourier transform [Yilmaz, 1987]. The Fourier transform is defined by the relation

$$\chi(\omega) = \int_{-\infty}^{\infty} x(t) e^{-i\omega t} dt \quad , \quad \text{eq. 5.7}$$

where ω is angular frequency, given by $\omega = 2\pi f$, where f is frequency and t is time.

When data are converted into the frequency domain (where frequency is the independent value) various data operations can be applied to the data such as filtering data on the basis of sound speed. Once unwanted data are removed, the inverse Fourier transform is applied to restore the data to the time domain for further processing.

5.4.3 – Data sorting

Digitized data are able to be sorted and thus manipulated in many ways based on information contained in the trace file headers. When samples and traces are acquired, they are done so time sequentially. That is, trace 1, sample 1, trace 2, sample 1, trace 3, sample 1, etc... But it is necessary for the purpose of visualizing acoustic impedance

boundaries to have data sorted *trace* sequentially. That is, trace 1, samples 1,2,3..., trace 2, samples 1,2,3..., etc. This conversion is done through a matrix routine, called demultiplexing and is one of the first steps in data processing [Sheriff, 1991]. Once traces are demultiplexed, they are ready to be further sorted in useful ways. It is common to begin with traces sorted as common shot gathers (Figure 5.5). Other ways in which data traces can be sorted are by common offset, common midpoint (between source and receiver), common reflection point or common depth point.

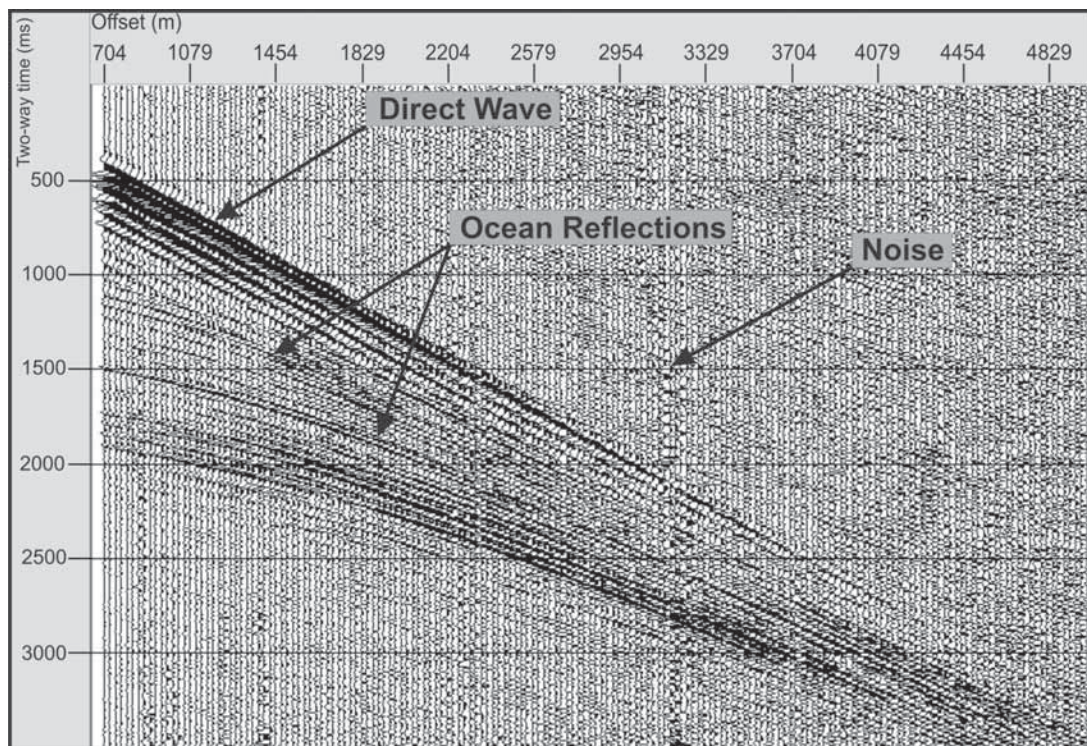


Figure 5.5 – Seismic data sorted by common shot showing major features: Direct Wave (coherent noise), Ocean reflections (hyperbolae) and noise. Axes are the source-receiver offset (horizontal) and two-way time (vertical). Two-way time is used in seismology as a proxy for depth. It is the time from source to reflecting interface and back to a given receiver.

Traces sorted by shot are now more geometrically representative of the subsurface. The linear direct wave is shown emanating from the source at the surface, appearing at later times at farther offsets. The acoustic impedance reflections are shown as hyperbolae and have a lower amplitude than the direct wave. To approximate a zero-offset seismic section we first sort the traces by their common midpoints. Ideally, we would like to

record acoustic reflections from directly below the source, so we can minimize unknowns such as anisotropic velocity variations in the ray path. But, in practice this is impossible due to the noise generated from the source distorting the signal arriving at the receiver. The common midpoint method therefore, allows us to image a point in the subsurface *as if* the source was directly above, halfway between source and receiver.

5.4.4 – Direct wave attenuation

Attenuation of the direct wave (the wave which travels along the most direct path from source to receiver without reflecting) is crucial in seismic oceanography. Whilst in marine MCS acquisition of the solid Earth, the direct wave can be safely removed along with the whole water column, this is not possible in seismic oceanography. The direct wave is present on all seismic records and, especially on near-offset traces, masks weaker reflections which themselves contain valuable information on oceanic fine structure.

Several methods have been tested on how to effectively attenuate the direct wave while maintaining signal integrity of the reflections. Firstly, since the direct wave is a linear wave, and reflections are hyperbolae, a simple, brute removal of the direct wave is possible with a top mute. This is not recommended, since it is still difficult to separate individual wavelets at near offset and results in their attenuation along with the direct wave.

The f-k (frequency-wavenumber) filter more effectively attenuates the direct wave. This is done by first transforming the data into the frequency-wavenumber domain (Section 5.4.2), whereby data can be filtered on the basis of sound speed. However, while the sound speed of the direct wave is less variable than reflected energy (because it travels near the surface from source to receiver without experiencing much change in speed as a function of depth or variations in thermohaline fine structure), oceanic sound speed variability is still rather subtle. This makes discrimination of the direct wave on the basis of sound speed an intricate and difficult procedure.

The Tau-p filter offers a better solution. It operates on the basis of the Tau-P transform which creates a slant stack (a seismic stacked section after applying a small time shift to traces) by transforming each sample in the time-offset domain into the Tau-P domain by a Radon transform, where Tau is the intercept time and P is 'slowness' or the reciprocal of phase velocity (sound speed). Since the Tau-P filter operates on the basis of dip, it can effectively remove the direct wave, which has a known dip. One disadvantage of the Tau-p procedure is that it can cause spatial aliasing of data [Stoffa et al., 1981].

The Eigenvector filter also presents a concise method of attenuating the direct wave. In this method, first a linear moveout correction is applied to the data. This operates more effectively on the linear direct wave than on hyperbolic moveout. Then, a Karhunen-Loeve process [Jones and Levy, 1987] is applied which decomposes the seismic data into eigenimages on the basis of which linear vs. hyperbolic events can be separated and removed. The eigenvector filter is also effective at removing random noise pre-stack (Figure 5.6).

5.4.5 – Frequency filtering

Filtering is done in the frequency domain to limit the frequency content of the data having the effect of improving the signal-to-noise ratio. Normally, band-pass filtering is designed to be zero-phase, meaning it does not modify the phase spectrum of the input traces, but only band limits its amplitude spectrum [Yilmaz, 1987]. Given an input seismic trace (time series) one applies a Fourier transform to resolve it into its individual frequency components. In the frequency domain the amplitude spectrum can then be shaped to contain the desired frequency characteristics. In general, seismic data usually contains some low and high frequency noise (e.g. ocean swell and electrical noise, respectively). These effects can be simply removed with this filter. In practice, a ramping taper at each end of the pass band taking the shape of a trapezoid is necessary to avoid 'ringing' caused by a sudden drop in frequency that is the result of a 'boxcar' shape in the amplitude spectrum [Yilmaz, 1987]. Band-pass frequency filtering can be very effective at removing specific ranges of random noise. However, caution should be exercised such as not to remove valuable signal, meanwhile. For noise that spans a larger range of the frequency spectra, other noise reduction methods may be preferable.

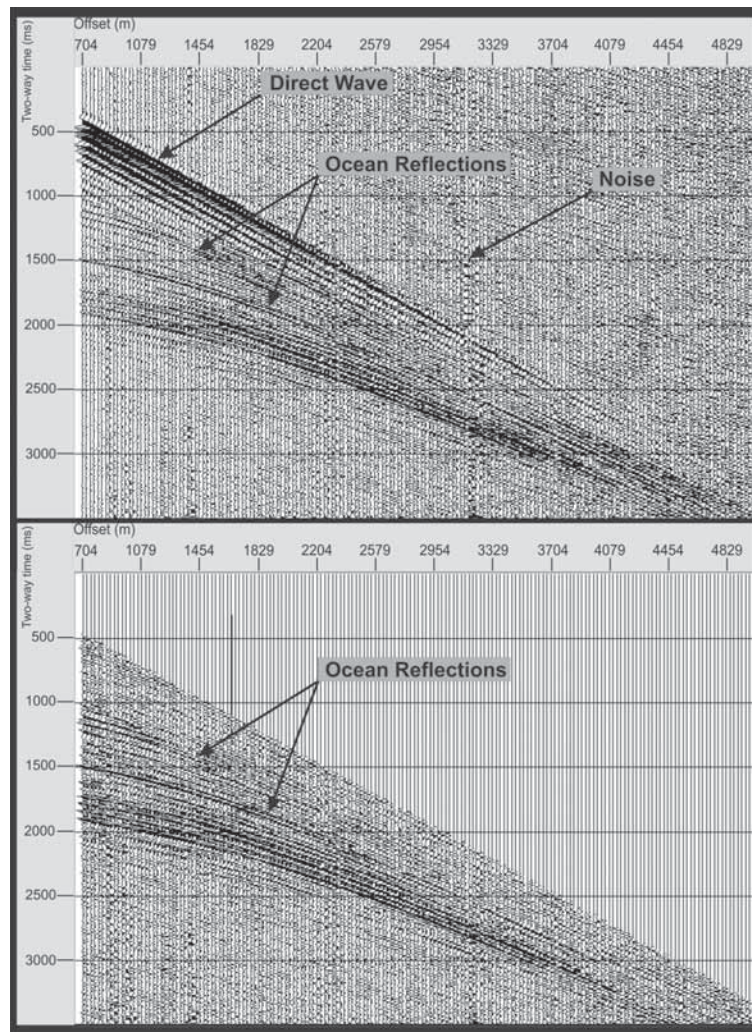


Figure 5.6 – Direct wave removal using the Eigenvector filter

5.4.6 – Spherical divergence corrections

Due to both geometrical spreading and physical attenuation in the medium, acoustic energy that has traveled through the water column and is later measured at the surface, is diminished. Samples which correspond to any given acoustic impedance boundary are reduced in amplitude by a factor that depends upon the ray path as well as the attenuation properties of the media themselves. Geometrical spreading in 'flat' media

(that is, for shallow depths relative to the diameter of the planet) follows the relationship, differentiated with respect to Snell's law

$$I = \frac{Pv_h \tan i_h}{x \cos i_o} \frac{d^2 t}{dx^2} \quad , \quad \text{eq. 5.8}$$

where, I is the energy density as defined as dE/dA , where E and A are Energy and Area of the wave front, respectively. P is the acoustic energy emitted per solid unit angle (dE/dU), v_h and i_h are the velocity and take-off angle at the focus and i_o is the incidence angle [Udías, 1999]. Geometrical spreading corrections are necessary therefore in the beginning of the processing sequence to account for the loss of seismic amplitudes which are inversely proportional to the depth to the reflection interface. Amplitude corrections for physical attenuation due to absorption by the medium through conversion to kinetic energy and heat loss can also be done by applying a correction with the attenuation factor, Q . However, water is a low-loss acoustic medium therefore physical attenuation corrections are not practically advantageous and do not significantly restore reflection amplitudes over geometrical spreading corrections alone.

5.4.7 – Deconvolution

Deconvolution is a wavelet shaping process designed to restore the original seismic wavelet as it was before the effect of linear filtering by the medium [Sheriff, 1991]. The primary objective of seismic data processing is to recover the reflection series from recorded traces such that they can represent the layering (acoustic impedance contrasts) in the earth, or in the water column. In addition to improving temporal resolution, deconvolution can suppress multiples (reflected energy that has reflected multiple times, thus delaying its arrival and appearing as a deeper reflection event). However, since deconvolution whitens the spectra as it increases resolution, it may also enhance high frequency noise. A recent publication by Biescas et al. [2010] reports significant improvement in seismic oceanographic signal quality after deconvolving the data. Papenberg et al. [2010] employed a deconvolution method that used the seismic source signal to compute amplitude reflection coefficients. This allowed inversion of the reflection coefficients for sound speed. From the sound speed estimates they could then

calculate temperature and salinity values directly, revealing the first 2D maps of temperature and salinity estimated from seismic data (Figure 5.7).

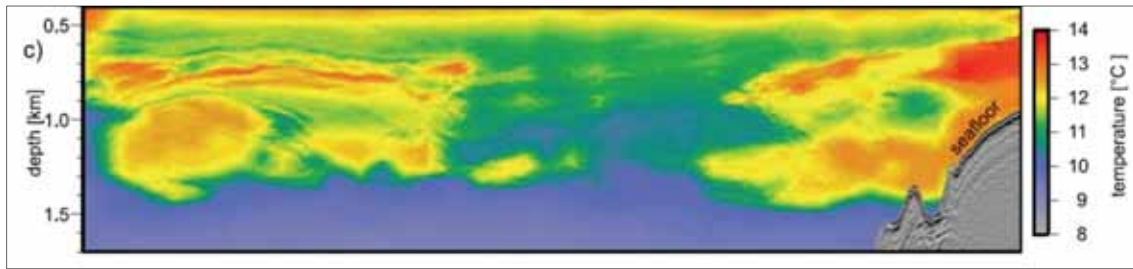


Figure 5.7 – 2D temperature distribution map estimated from seismic data. From Papenberg et al. [2010].

5.4.8 – 'Velocity analysis' and normal moveout correction

For a given CMP gather, in order to correct for the effect of normal moveout, that is, the effect of increasing reflection travel time with longer offset receivers (traces), one needs to apply an appropriate shift in 'stacking velocity' to flatten the hyperbolic reflectors as if the receivers were all located at zero-offset. Stacking velocity is the chosen velocity function used for NMO correction that yields the best stacking response [Hatton et al., 1986]. In this way stacking velocity corrections are somewhat cosmetic. However, it does approximate the NMO velocity. That is, while the NMO velocity is based on the small spread hyperbolic travel-time [Taner and Koehler, 1969], stacking velocity is based on the hyperbola that best fits the data over the entire spread length [Yilmaz, 1987]. The numerical representation of normal moveout correction is given as

$$\Delta t_{nmo} = t(0) \left\{ \left[1 + \left(\frac{x}{v_{nmo} t(0)} \right)^2 \right]^{1/2} - 1 \right\} \quad , \quad \text{eq. 5.9}$$

where $t(0)$ is the two-way travel time along a vertical path, x is offset, and v_{nmo} is the sound speed of the medium before the reflecting interface. Sound speed varies vertically and horizontally, so it is necessary to pick a vertically varying velocity function at various locations along the profile to correct for normal moveout (Figure 5.8). Fortin and Holbrook [2009] analyzed seismic oceanography data for the proper sound speed requirements necessary for optimal imaging. They tested four sound speed models: a)

constant sound speed of 1500 m/s, b) a sound speed profile from the Levitus world ocean database, c) sound speed derived from 17 XBT profiles and d) standard stacking 'velocity analysis'. It is clear that a constant sound speed is not appropriate. Although some features can still be delineated, there are still significant improvements possible through other methods. Data from the historical database showed slight improvements in signal-to-noise ratio and allowed a 7-fold increase in the auto-tracking of reflectors. Both the XBT generated sound speed profile and the handpicked profile showed nearly a doubling of signal-to-noise ratio over the Levitus data, but the handpicked profile allowed auto-tracking of more reflectors. Figure 5.8 shows a typical 'velocity analysis' interactive process.

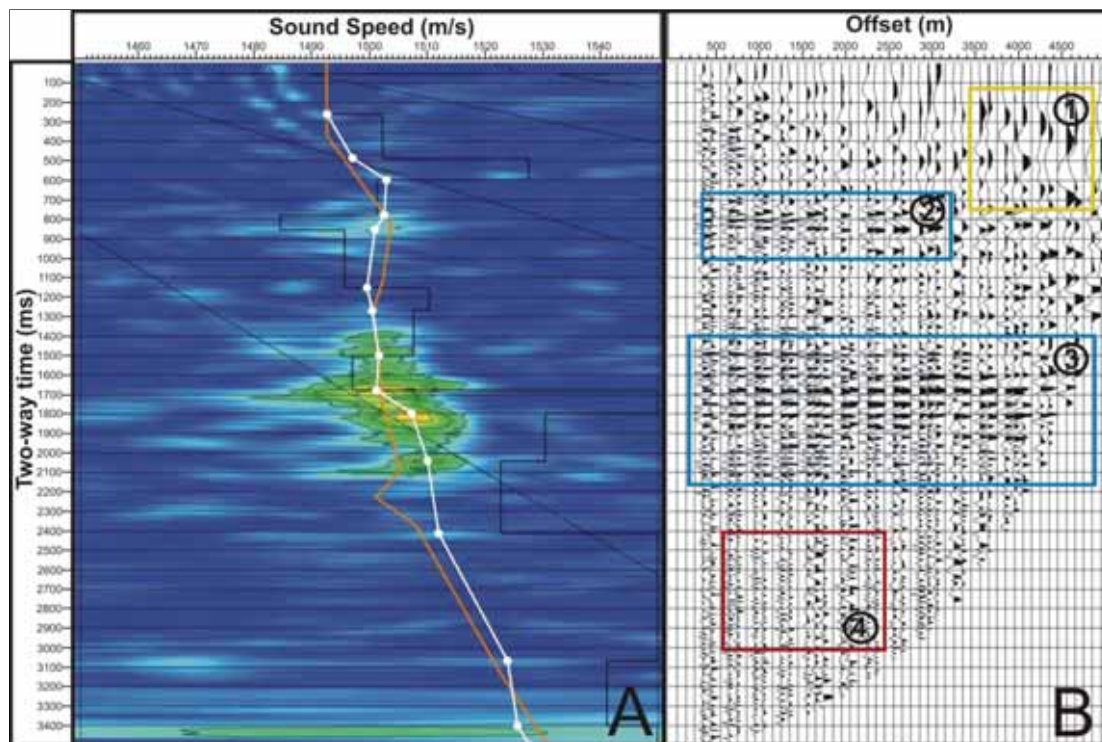


Figure 5.8 – Semblance Velocity Analysis. **Panel A:** Semblance Gather: sound speed adjustments are made by interactively modifying sound speed as a function of two-way time (a proxy for depth). White line is sound speed profile showing 'picks'; Orange line is a guideline based on an adjacent CMP gather. Black blocky line shows interval velocity (sound speed within a layer); Black linear lines are guidelines to prevent non-physically realistic picks; Green/Yellow/Orange/Blue pattern is the semblance spectra based on signal coherency across adjacent CMP traces. **Panel B:** CMP gather: 1) NMO stretch effect; 2),3) signal that will constructively interfere; 4) 'noise' that will destructively interfere.

Compared with such analysis of solid Earth data, where sound speed can vary from approximately 2000 m/s up to 8000 m/s, there are only very subtle sound speed changes within the ocean (on the order of 50 m/s differences). However, velocity analysis is still sensitive to these changes and a significant improvement to the final section can be made through careful analysis.

An undesirable side-effect of velocity analysis is NMO stretching. While correcting for normal moveout, samples are differentially shifted, producing a non-linear distortion in wavelet shape [Hatton et al., 1986]. This effect is mostly noticeable at far offsets because it is directly related to the amount of static shift. NMO frequency distortion is quantified as

$$\frac{\Delta f}{f} = \frac{\Delta t_{\text{nmo}}}{t(0)} \quad , \quad \text{eq. 5.10}$$

where f is the dominant frequency, Δf is the change in frequency and Δt_{nmo} is given by Equation 5.9.

5.4.9 – CMP stacking

After the normal moveout correction, traces are summed, or 'stacked' so that trace coherency constructively interferes and incoherent traces destructively interfere resulting in one summed trace to represent a common midpoint. The redundancy of many common midpoints increases the signal-to-noise ratio. Stacking compresses the offset dimension thereby reducing the data volume to the plane of a zero-offset section [Yilmaz, 1987]. Stacking is perhaps the most common operation and is performed almost always. It is such a defining procedure of seismic data processing that data are grouped into pre-stack and post-stack. Pre-stack data potentially has all possible information available after digitization. Post-stack data is intrinsically sub-sampled. Much less data exist after stack than before stack because of the trace summing process. It is crucial before stack to obtain the best possible signal-to-noise ratio such that no valuable signal is lost during stacking. Quantitatively, the mean sample value for a

given two-way travel-time is calculated and we define the sample values on trace i as $a_i(t)$, its mean given by the relation

$$A(t) = \frac{1}{N} \sum_{i=1}^N a_i(t) \quad . \quad \text{eq. 5.11}$$

5.4.10 – Migration

Sheriff [1991] describes seismic migration as an inversion operation involving rearrangement of seismic information elements such that events are displayed at their true subsurface locations. Migration moves dipping reflections up-dip and collapses diffraction hyperbolae. It adjusts dipping interfaces because energy reflected from dipping horizons does not arrive at the same time as energy from a horizontal interface for any given offset. Therefore, in the physical interpretation of seismic data, migrated data correctly positions reflections. Ideally, migration requires a priori knowledge of the sound speed field of the media in question, but in practice this is not known and must be arrived at iteratively through velocity analysis. Co-located and simultaneously recorded in situ oceanographic sound speed measurements (such as XBTs, XCTDs – Chapter 6) have the potential to more accurately represent the migration sound speed field than velocity analysis iterations alone.

5.4.11 – General considerations

The above description of seismic processing operations is highly abridged. For further details of seismic data processing the reader is referred to two texts in particular: Seismic Data Processing [Yilmaz, 1987; 2001] and Seismic Data Processing - Theory and Practice [Hatton et al., 1986]. Both texts are aimed at audiences of professionals in the hydrocarbon industry. At this point there is no definitive reference book on seismic processing for seismic oceanography. However, this thesis may serve as general starting point for the uninitiated researcher whom may wish to follow some of the references herein.

Challenges still exist in seismic oceanography data processing which need investigation. One such challenge is dynamics. For a moving ship and a moving target (relative to the seafloor), the acquisition is not well constrained. Klaeschen et al. [2009] addressed this

through making the first estimate of the movement of reflectors in the water column from seismic data. The methodology was based on using true-amplitude pre-stack time migration to increase the lateral and temporal resolution by reducing the Fresnel zone. The amplitudes thereby correspond to impedance contrasts. For migration of solid Earth data, the geometry can be measured precisely. However, for a dynamic ocean this is not possible to the same degree due to the spatial and temporal movement of thermohaline finestructure. Thus, while for the solid Earth, given a known geometry, an optimum sound speed field can be arrived at, for the ocean, the reverse is done. That is, given a constrained sound speed field (arrived at independently from oceanographic data), the optimum geometry for a dynamic fluid can be calculated and therefore, its motion. More research into dynamics is an important step in uncovering the still only partially understood mechanisms behind ocean dynamics, and therefore, mixing and larger scale circulation.

5.5 – Interpretation

Accurate interpretation of seismic oceanography data is the desired outcome of any acquisition and processing scenario. As mentioned, caution needs to be exercised in this regard for various reasons, but crucially because of the dynamic nature of the ocean on time scales relative to acquisition and, thus the transience of reflectors (e.g. Géli et al. [2009]; Klaeschen et al. [2009]; Chapter 3). As in studies of the solid Earth, where a geologist with specialized knowledge may contribute to interpretation, physical oceanographers are needed to properly interpret MCS 'reflectivity maps' of the ocean.

Interpretation is a key point at which seismic oceanography is cross-disciplinary. So, in addition to it being considered a tool of physical oceanography one sees the merging of two disciplines that may eventually result in the emergence of a comprehensive discipline unto itself, particularly if one considers the participation of other branches of oceanography (e.g. marine biology or chemical oceanography).

The next chapter further addresses interpretation in the context of the structures and processes of interest to physical oceanographers.

CHAPTER 6

Physical Oceanography

I was like a boy playing on the sea-shore, and diverting myself now and then, finding a smoother pebble or a prettier shell than ordinary, whilst the great ocean of truth lay all undiscovered before me.

– Isaac Newton

6.1 – Introduction

The ocean has always been the focus of much respect and curiosity. Since antiquity it has provided us sustenance, transportation and more, yet at depth it is largely unexplored. To the very first ocean scientists it likely seemed unexplorable. Indeed many unsuccessful attempts were made to measure its depth but for lack of a sufficiently long rope.

The ocean covers more than 70% of the Earth's surface and although it is much less in volume than the atmosphere, it carries roughly an equivalent amount of heat due to its relatively high value of specific heat [Thorpe, 2005]. This fact alone makes ocean circulation of very great climate influence. The popular, but oversimplified, illustration of this is the Gulf Stream's effect on the milder climate of Europe vis-a-vis similar latitudes in Labrador, for instance [Seager, 2006].

Ocean circulation is the system of large scale currents that distribute its mass. It is driven mainly by the wind and secondarily by tidal forcing [Wunsch, 2002]. The wind is driven by uneven solar heating of the Earth as it rotates between day and night. Tidal forcing is mainly a result of the gravitational pull of the Sun and Moon. However, it is also a function of sea level, which varies depending on factors such as the global cryosphere extent, a topic of increasing interest with respect to global warming. In addition, meteorological tides can be measured in the presence of storm systems. The atmosphere and ocean are coupled in this and many other respects and on a large scale function like a single dynamic, highly stratified rotating fluid. One cannot speak about climate independent of the ocean.

It is well beyond the scope of this thesis to present a complete treatise of physical oceanography. However, since the underlying basis for research into seismic oceanography is to help elucidate physical oceanographic structures and processes, it is prudent to start this chapter by acknowledging that seismic oceanography is only one of many tools within the discipline of physical oceanography. Seismic oceanography is a new and potent tool, but like any tool it is limited. Thus, this chapter discusses: 1) some of the conventional tools of physical oceanography, in addition to 2) the structures and 3) the processes that are presently amenable to seismic ensonification.

6.2 –Tools of physical oceanography

6.2.1 - *In situ probes*

The development of the CTD (Conductivity-Temperature-Depth) cast in 1955 led to accurate direct probing of the ocean [Ingmanson and Wallace, 1995]. The CTD allowed the first direct Eulerian measurements of variation in physical properties with depth in the ocean by providing a measurement of salinity (conductivity), temperature and depth (pressure). Expendable probes are also very common because they allow an Eulerian measurement of physical ocean properties at fixed points in space as a function of depth and are deployable as the ship is moving, which allows for their simultaneous deployment with seismic acquisition. A much denser horizontal grid of data can be acquired with expendable probes, whereas the CTD requires the ship to be stopped while it is lowered and raised. The Expendable Bathythermograph (XBT) (Figure 6.1) is capable of measuring vertical resolutions as small as 65 cm and temperature variations as small as ± 0.07 °C [Boyd and Linzell, 1993]. The vertical resolution of in situ probes is much better than that of seismic data, one of the main complementary advantages of seismic data being its *horizontal* resolution. Expendable CTDs or XCTDs are also sometimes deployed along with XBTs, but are rather more expensive and less reliable than XBTs. However, the conductivity measurement gives an estimate of salinity which can then be used as a factor to constrain sound speed estimates.

6.2.2 - *Float measurements*

In addition to in situ Eulerian measurements of ocean properties, Lagrangian measurements, where a measuring device follows the trajectory within the fluid, are also informative. Beginning in 1993 (eg. Bower et al. [1997]), as part of the AMUSE (A Mediterranean Undercurrent Seeding Experiment) project, RAFOS floats (sonically detectable, sub-surface instruments) were deployed and were tracked acoustically for eleven months. This experiment showed the path of meddies and the Mediterranean Undercurrent and further established the significance of the Undercurrent as having an important role in the broader Atlantic ocean (Figure 6.2).

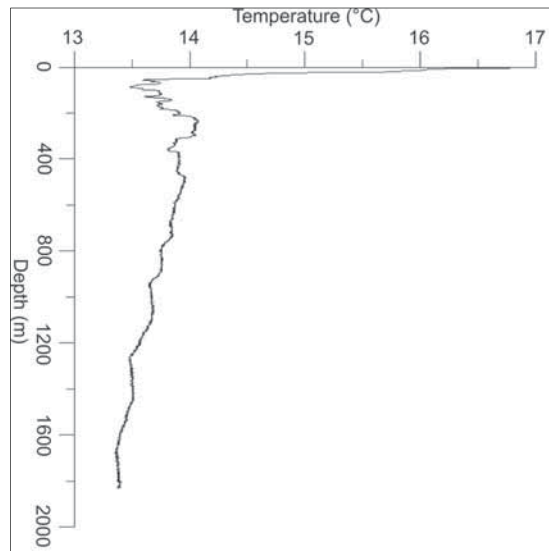


Figure 6.1 - XBT profile from the Tyrrhenian Sea showing characteristic temperature steps (thermohaline staircase). Temperature drops quickly in the upper ocean then shows a small increase before the staircase formation beginning at approximately 700 m.

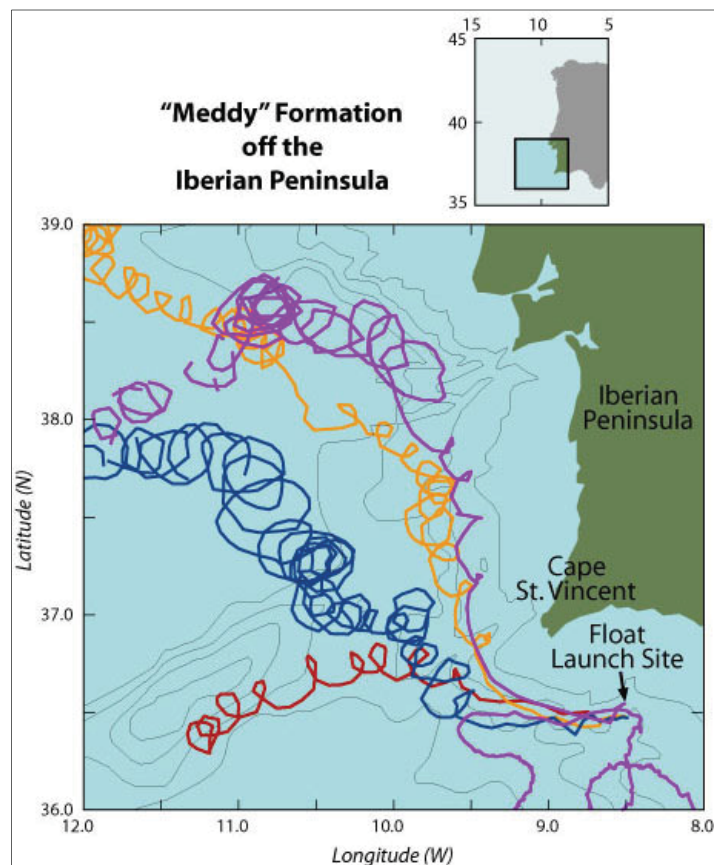


Figure 6.2 - Meddies tracked by RAFOS floats – courtesy, Jayne Doucette, Woods Hole Oceanographic Institution.

6.3 – Structures

6.3.1 – Thermohaline staircases

Thermohaline staircases are regular, well-defined, step-like variations in vertical temperature and salinity gradients that form when temperature and salinity increase with depth and nearly compensate with density [Kelley, 1984]. Turbulent mixing can disrupt the regular step-like structures, so they are typically found in regions where the Prandtl number (the ratio of viscous to thermal diffusion rates) is near unity and turbulent mixing is unusually weak [Merryfield, 1999]. Therefore, isopycnal stratification is more static than in regions dominated by turbulence. Morell et al. [2006] studied an eddy in the Caribbean Sea. Its associated thermohaline staircases were reported to have formed from an interplay of two mechanisms: lateral property contrasts and shear within the eddy. However, they admit that their interpretation is less than definitive due to 'coarse horizontal sampling', which is one of the principal advantages of MCS profiling.

Staircases have been identified in several places worldwide using seismic oceanography (e.g. Biescas et al. [2010], Fer et al. [2010]). They have been known for some time to exist in the Tyrrhenian Sea, a deep basin within the Mediterranean Sea characterized by a circumferential current and stable central stratification (e.g. Zodiatis and Gasparini [1996]; Sparnocchia et al. [1997]). Thermohaline staircases were detected oceanographically (using XBT probes) and seismically during the author's recent cruises in the region [Ranero et al., 2010]. Oceanographic probes showed clear step-like structures that were only present in the deepest parts of the basin and increased in step riser-width with depth (Figure 6.3).

6.3.2 – Eddies/Meddies

Eddies are quasi-spherical lenses of fluid that form in the presence of diapycnal mixing and turbulence where isopycnals are disturbed. Thorpe [2005, p.35] describes one mechanism of eddy generation in four stages: a) a uniform density gradient is present, given by

$$\rho = \rho_0 \left(1 - \frac{N^2 z}{g}\right) \quad , \quad \text{eq. 6.1}$$

where ρ is density, N is the buoyancy frequency, z is the upward vertical measured from the mean depth of the mixed region; and g is the acceleration due to gravity; b) turbulence, leads to; c) homogenization of a density patch; and d) due to the horizontal pressure gradient, the mixing region is forced to spread laterally, whilst, to conserve its volume, it collapses vertically and intrudes into the surrounding water along similar isopycnal surfaces. During the process of turbulent mixing and intrusion, internal waves may be generated that then radiate into the surrounding quiescent fluid. The spreading of the mixed region causes dispersion of particles along isopycnal surfaces, whereby the rotation of the Earth (and the resulting Coriolis force) causes the mixed region to rotate anti-cyclonically.

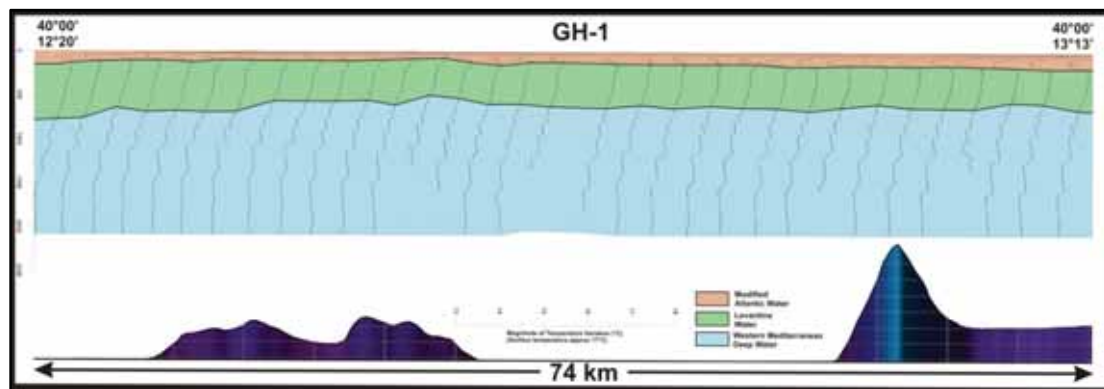


Figure 6.3 - Map of the lateral distribution of XBT profiles in the Tyrrhenian Sea. Three main water masses are identified: a) Modified Atlantic Water (pink), b) Levantine Water (green) and c) Western Mediterranean Deep Water (blue), which is characterized by staircase formation. From Ranero et al. [2010].

Meddies (or, Mediterranean eddies) are large (40-150 km in diameter), coherent anti-cyclonic lenses of Mediterranean outflow water with characteristic salinities of approximately 36.5 psu and maximum temperatures of around 13°C [Richardson et al. 2000]. Some meddies preserve a double-core structure typical of the Mediterranean Undercurrent [Zenk, 1970] from which they originate. Meddies translate southward and westward from Cape St. Vincent (Portugal) [Richardson et al., 1989], and northward, along the coast of Iberia [Buffett et al., 2009], while diverging from the Mediterranean Undercurrent.

Meddies have become favorite targets of seismic oceanographers (e.g. Biescas et al. [2008]; Krahnmann et al. [2008]; Buffett et al. [2009]; and Pinheiro et al. [2010]) due to their spatial extent, high property contrasts as well as their oceanographic significance for the distribution of conservative physical properties in the eastern North Atlantic ocean where they play an important role in the transport of salt and heat [Armi et al., 1989]. Buffett et al. [2009] reported that meddies further from their Strait of Gibraltar source appear more internally well mixed, whilst maintaining their overall form (Figure 6.4).

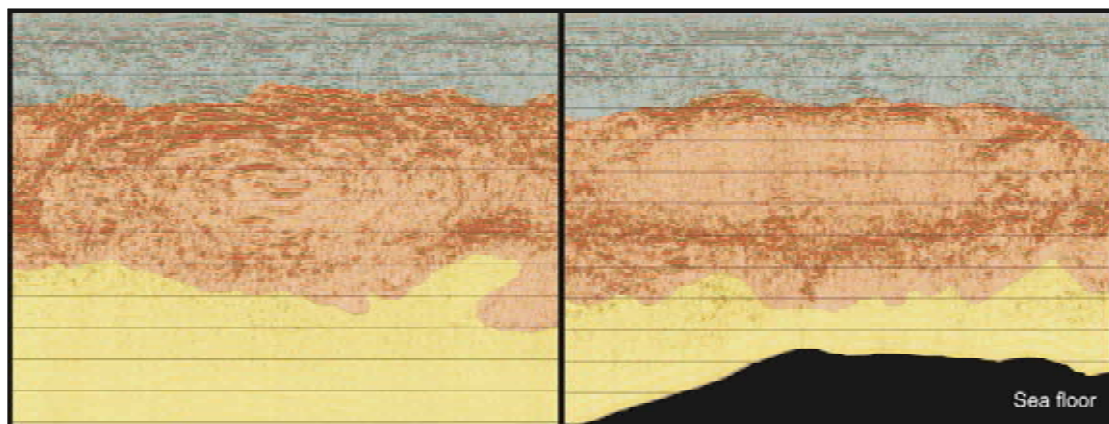


Figure 6.4 - Comparison of the internal structure of two meddies. The left panel shows a meddy near Cape St. Vincent (Line IAM-3); the right panel shows a meddy that has been displaced downstream by the Mediterranean Undercurrent (Line IAM-11). Note the lack of internal structure in the displaced meddy compared to the meddy near Cape St. Vincent. This result is likely due to the internal homogenization of the displaced meddy through turbulence and mixing processes. Meddy sizes are proportional. See Appendix 2 for complete seismic profiles and geographical locations. Modified from Buffett et al. [2009].

6.3.3 – Fronts

As in the atmosphere, fronts within the ocean are clearly visible due to strong property contrasts. Fronts can be seen whenever there are stronger than normal property contrasts, but they may be formed due to the interaction of internal waves with the continental shelf, where isopycnals are steepened [Thorpe, 2005]. Holbrook et al. [2003] made the first seismic identification of an oceanic front, plausibly as a result of the interaction between two water masses (Figure 6.5).

Nakamura et al. [2006] made seismic observations of the Kuroshio extension front near Japan. They conducted the survey along with the deployment of physical oceanographic

measurements confirming the correlation to the former. Thorpe [2005] reports that in addition to fronts which form as a result of the steepening of isopycnals at a continental shelf, temperature contrasts as small as 5 mK can be observed in fronts. Thermal fronts with temperature contrasts this small are only slightly beyond the present limit of seismic detection (Nandi et al. [2004] found that seismic oceanography could detect temperature contrasts at least as small as 30 mK).

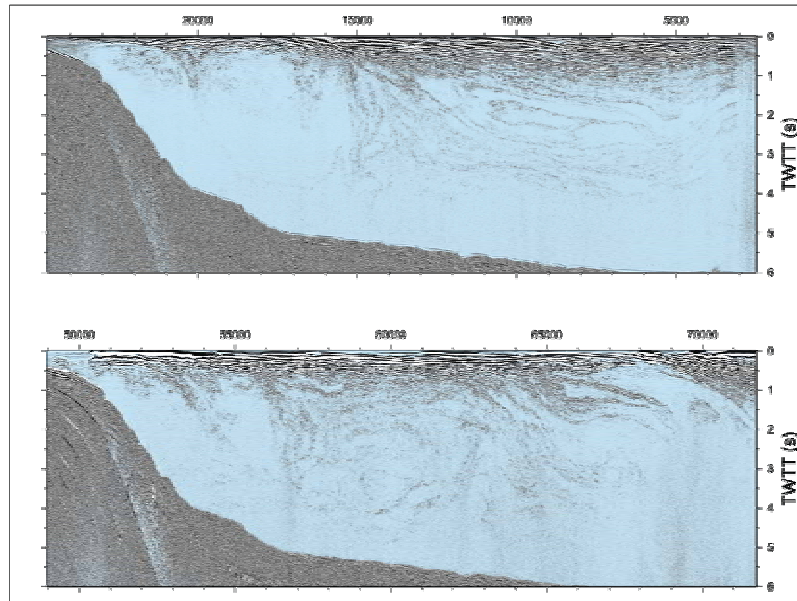


Figure 6.5 - The first seismic images of an oceanic front showing the interaction between two water masses near the Grand Banks of Newfoundland (the North Atlantic Current and the Labrador Current). Horizontal axis is CMP number (section 5.3.2) and the vertical axis is two-way-travel time in seconds. From Holbrook et al. [2003].

6.3.4 – Currents

Currents can be practical targets for seismic oceanography, especially at their boundaries where they must entrain and otherwise interact with surrounding waters. The Mediterranean Undercurrent is a good example of a strong current with sharp property contrasts between temperatures and salinities. Buffett et al. [2009] (Chapter 1) seismically imaged portions of the Mediterranean Undercurrent along its flow path. They reported that within the current itself, property contrasts diminished as a function of distance from the Mediterranean Water source, but observed that at the apparent edges of the current, property contrasts (and thus, acoustic impedance contrasts) remained strong, especially where the Mediterranean Undercurrent entrained and interacted with the North Atlantic Central Water. Currents are important oceanographic

structures because, especially on a large scale, they distribute heat, salt and mass around the planet, affecting climate. Current circulation between ocean basins, in bays, harbors, inlets and fjords, where circulation is regular on a seasonal, monthly or diurnal basis [Trevorrow, 2005] may provide interesting areas of study. Circulation in the Tyrrhenian Sea is a good example of a boundary current enclosing a deep basin. Here, circulation is circumferential with little mass flux below 700 m into the deepest parts of the basin where the deep water residence time is on the order of 30 years, whereas shallower currents circulate in 2-3 years [Zodiatis and Gasparini, 1996]. Ongoing seismic oceanography studies by the author and others in the Tyrrhenian Sea delineate stable staircases in the central portion of the basin while showing the circulation current characterized by turbulent mixing in some of the shallower, boundary waters.

6.4 - Processes

6.4.1 - Mixing

Ocean mixing is the process by which different water masses combine. It can occur on the largest scale of global circulation to the smallest molecular scales of mixing. Mixing acts to smooth property distributions in the ocean of heat, salt and other chemicals. It can occur along (lateral mixing) or across (diapycnal mixing) isopycnals. Stern [1967] notes that where instabilities develop, salt can be easily transported along isopycnals. Diapycnal mixing is more difficult to occur because the energetics involve moving deeper, heavier water masses above lighter, more buoyant ones, that is, motions are inhibited for diapycnal mixing simply due to the pressure gradient. Ruddick [1992] found that the energy needed to drive intrusive motions indicated double diffusive convection as a possible mechanism. Double diffusive convection describes the form of convection driven by adjacent fluids which have different densities and diffusion rates. The density gradient is the result of the combination of differing compositions (i.e. salinity) and temperatures. Since heat diffusion occurs approximately one hundred times faster than molecular diffusion [Thorpe, 2005], features such as 'salt fingers' occur [Stern and Turner, 1969], where warm salty water overlies cold fresh water. Consider a small parcel of warm, salty water forced to sink into a colder fresher zone. The sinking plume will lose its heat to the colder water before losing its salt, thus becoming denser

than the water around it and sinking further. Similarly, if a small parcel of cold fresh water is displaced upwards, it will gain heat by diffusion from the surrounding waters, which will then make it lighter than the surrounding waters, and cause it to continue to rise. The fact that salinity diffuses much less efficiently than temperature, then paradoxically results in a process that mixes salinity more efficiently than temperature. Salt fingering thereby contributes to diapycnal mixing in the oceans, which helps regulate the gradual overturning circulation of the ocean that in turn strongly affects climate. Mixing can also take place as an effect of tidal action and internal waves [Thorpe, 2005]. The extent of the contribution of marine organisms to ocean mixing is still unknown. Katija and Dabiri [2009] recently reported the mixing effect of jellyfish through their motions to be a significant contribution to ocean mixing and nutrient transport. Undoubtedly, mixing occurs across a range of scales due to the propulsion of animals and the stirring in their wakes, but the degree to which this affects mixing globally is still uncertain.

6.4.2 - Turbulence

Thorpe [2005] defines turbulence as an energetic, rotational and eddying state of motion that generates relatively large gradients of velocity over small scales (1 mm to 1 cm), thereby promoting the conditions in which viscous dissipation transfers its kinetic energy to heat. It produces dispersion of material and transfers momentum, heat and solutes at rates higher than molecular processes alone. Reynolds [1883] made the first laboratory observations of turbulence, noting that for a jet of dyed liquid entering a tube of water, while initially laminar in form, it transitioned to a turbulent flow as the velocity of the jet was increased, thus mixing all at once with the surrounding water, showing distinct curls and eddies. Of course this controlled laboratory experiment is not possible in the ocean, where many other factors are at play and where observations are affected by many unseen or subtle variations in the physical properties of water. One example of the transition from stability to turbulence is that of a breaking wave. Indeed, breaking internal waves occur within the ocean. Turbulence and mixing are closely related processes in which zones of elevated turbulence are prone to mixing, at least on a small scale. However, mixing and interleaving of stratification along isopycnals need not strictly be turbulent. Diapycnal mixing is more likely to occur at smaller scales,

involving turbulent processes in some way due to the fact that isopycnals are thereby disturbed.

6.4.3 - Dynamics

Ocean dynamics poses a difficult challenge for seismic oceanography in that MCS profiling had been exclusively developed by the hydrocarbon industry to image sub-sea floor media, a regime which is comparatively static with respect to the ocean, where currents are typically on the order of 0.5 ms^{-1} and where internal waves can propagate on the order of 1 ms^{-1} . These velocities are sufficient to prevent the generation of a snap-shot type seismic image, as is characteristic for study of the solid Earth. That is, ocean dynamics necessitate only a quasi snap-shot of the motion of interior ocean property contrasts using conventional MCS. During the GO project acquisition stage in April and May 2007, in order to test the viability of seismic derived ocean dynamics, several repeat passes were made over the same geographical location at intervals ranging from 30 minutes to 12 hours. During one particular repeat survey with an opposite azimuth, apparent wavelength changes of reflectors were noticed that were explained by a Doppler-like effect [Klaeschen et al., 2009]. By constraining the ship's velocity variable, it appeared that the motion was singularly related to reflector (and therefore, property contrast) translation, the magnitudes and vectors of which were estimated (Figure 6.6).

This first attempt at remotely estimating the velocity of subsurface finestructure clearly demonstrates the utility of MCS profiling to oceanographers. Chapter 3 illustrates another method of visualizing the movement of reflectors without having to do repeat acquisition transects. The caveat being the requirement of a high signal-to-noise ratio and a sufficiently long recording streamer to allow enough time for noticeable movements. These methods and others illustrate the importance of being able to glean more than just positional information from seismic data.

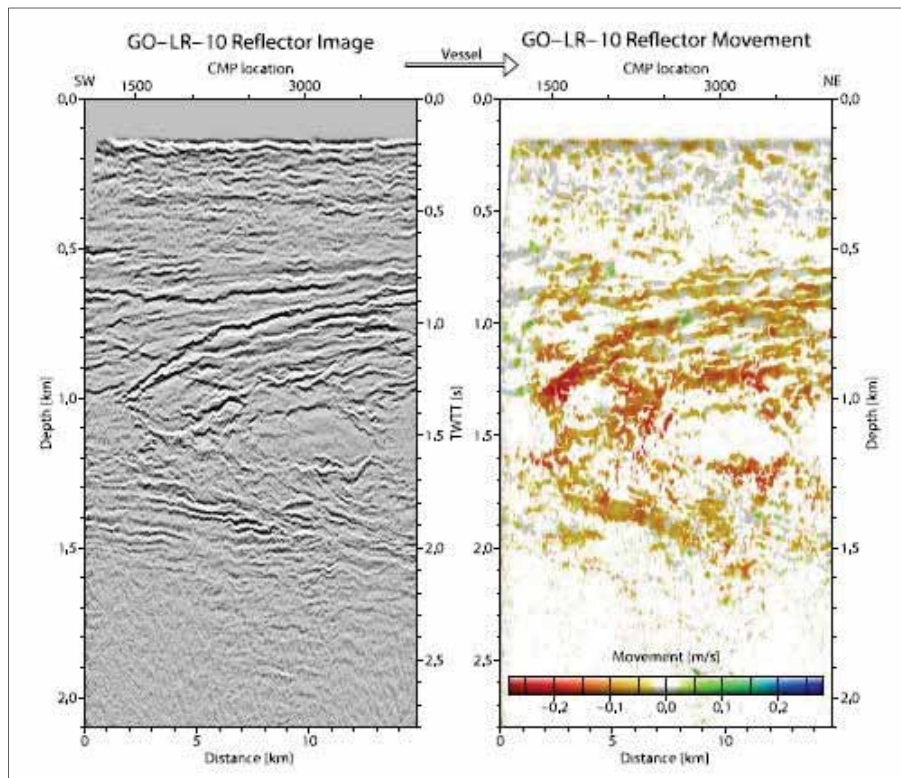


Figure 6.6 - Seismic reflector dynamics. Left panel shows final stacked seismic image of a portion of a meddy. Right panel shows movement velocity derived as an inversion parameter. Movement velocity is indicated by a color scheme. From Klaeschen et al. [2009].

6.4.4 - Internal waves

Internal waves are gravity waves in the interior of the ocean (or generally any fluid) that arise from changes in hydrostatic equilibrium, that is, the balance between gravity and buoyancy [Thorpe, 2005]. Internal waves may have different sources, caused by oscillations in atmospheric pressure, wind, tidal forces, or through interaction with the seafloor [Miropol'sky, 2001]. Curiously, Rhie and Romanowicz [2004] recognized a background seismic signal oscillation that could not be explained by summing together the global occurrence of all earthquakes. The mechanism for the so-called 'hum' was explained as atmosphere-ocean-seafloor coupling, probably through the conversion of storm energy to oceanic infragravity waves interacting with seafloor topography. If correct, the 'hum' might provide another mechanism for internal waves and substantiate the importance of the latter with respect to their influence on climate. In this respect, internal waves drive turbulence and diapycnal mixing [Garrett, 2003] and play an important role in the distribution of biomass and nutrients [Echevarría et al., 2002].

Holbrook and Fer [2005] first used seismic oceanography to estimate internal wave spectra in the boundary layer between the Norwegian Atlantic Current and the Norwegian Sea Deep Water. They found that horizontal wavenumber spectra derived from seismic data matched well with the Garrett-Munk tow spectra, which describes the internal wave field. Krahnemann et al. [2008] used seismic oceanography to quantify internal wave energy. Interestingly, they found variations in the internal wave field on either side of the Gorringer Bank, a large seamount which is crossed by Mediterranean Outflow Water. They speculated that this may be due to the presence of a meddy on one side.

This volume contains two contributions to the study of internal waves using seismic oceanography: Chapter 2 introduces the method of Stochastic Heterogeneity Mapping to seismic oceanography and estimates ranges of scale lengths of oceanic features such as internal waves. Chapter 3 shows the application of a customized processing scheme to visualize animation of internal waves in near-real time.

6.4.5 - Topographic interaction

Interaction with topographic relief is another important contribution of MCS profiling to oceanography. Internal waves can be generated as 'lee waves' where stratified water moves past a natural obstacle such as a seamount [Thorpe, 2005]. Biescas et al. [2010] seismically analyzed thermohaline staircases in interaction with a seamount (the Gorringer Bank in the Gulf of Cadiz). It is clear from the image (Figure 6.7) that otherwise stable thermohaline staircases are disturbed by interaction with the seamount. Biescas et al. [2010] interpret the distortion of staircase layers on the impinging side of the seamount as due to turbulent vertical mixing generated at the boundary of the abrupt topography. Holbrook and Fer [2005] showed a similar distortion effect where isopycnals interact with slope topography. That is, at some distance from the slope, reflectors were more continuous, whereas adjacent to the slope, reflectors 'pile up' creating an undulating pattern (Figure 6.8).

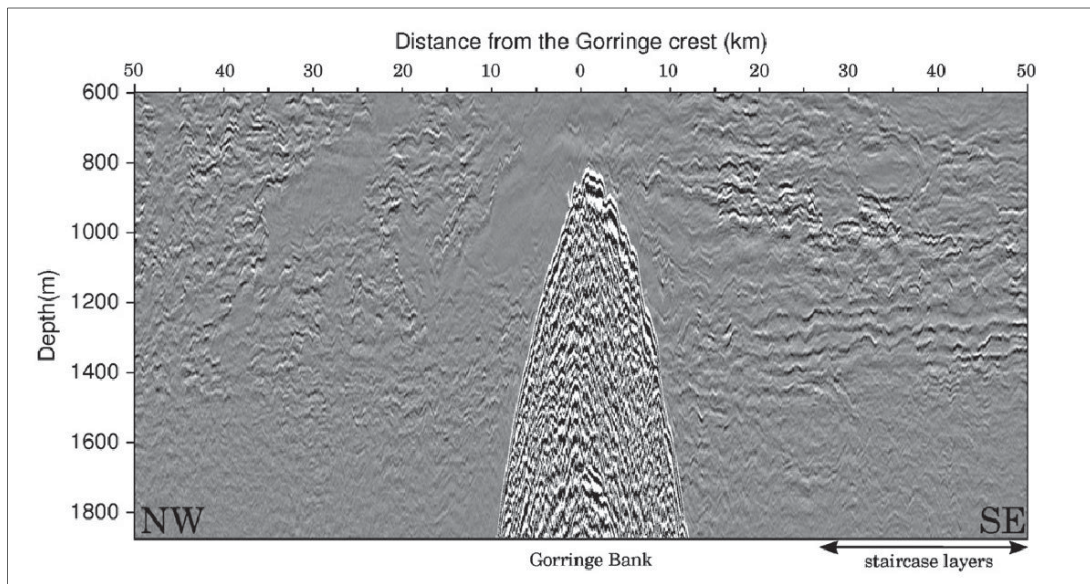


Figure 6.7 - Interaction of thermohaline staircases with the Gorringe Bank (an isolated seamount in the Gulf of Cadiz). Flow direction is approximately from right to left. Reflectors seem to 'ramp up' on the seamount in a similar manner that a meteorological front interacts with a mountain. Notice the 'rain shadow' analog on the NW side of the bank as reflectors lose their lateral coherence and are forced above the seamount, remaining less coherent on the NW side. From Biescas et al. [2010].

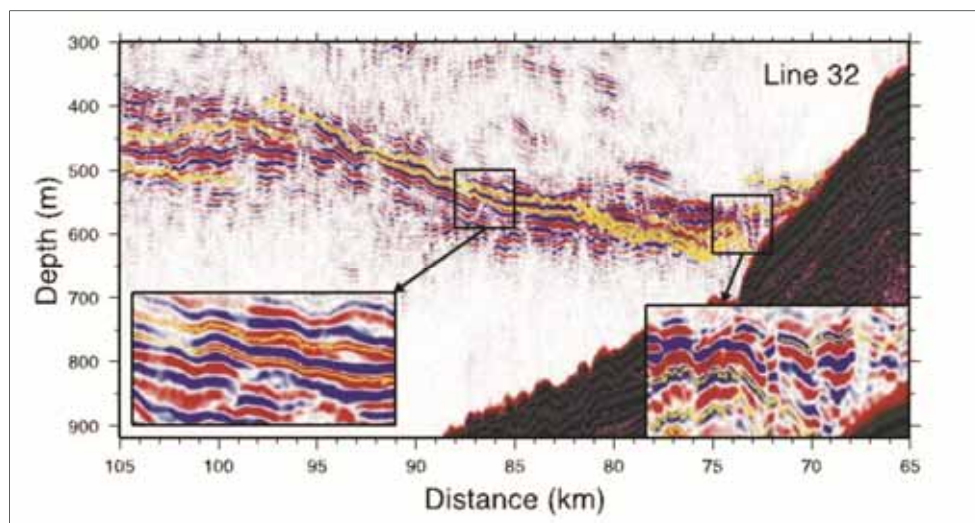


Figure 6.8 - The interaction of reflectors with topography. Note the continuity and undulating nature of the left and right inset boxes, respectively. Yellow lines show autopicked reflector interfaces used in spectral analysis. From Holbrook and Fer [2005].